Plant Biotechnology Journal
Open Access

Plant Biotechnology Journal (2022) **20**, pp. 1648–1650 doi: 10.1111/pbi.13884

Brief Communication

Spatial transcriptome analysis on peanut tissues shed light on cell heterogeneity of the peg

Yiyang Liu[1,†], Chunhua Li[2,†], Yan Han[1], Rongchong Li[1], Feng Cui[1], He Zhang[2], Xiaoshan Su[2], Xiawei Liu[2], Guoxin Xu[3,*], Shubo Wan[1,*] and Guowei Li[1,*]

[1]*Institute of Crop Germplasm Resources, Shandong Academy of Agricultural Sciences, Ji'nan, China*
[2]*BGI-Qingdao, BGI-Shenzhen, Qingdao, China*
[3]*Institute of Wetland Agriculture and Ecology, Shandong Academy of Agricultural Sciences, Ji'nan, China*

Received 9 January 2022;
revised 25 June 2022;
accepted 27 June 2022.
**Correspondence* (Tel 0086-531-66658902; fax 0086-531-66658156; email liguowei@sdnu.edu.cn (GL); Tel 0086-531-66659295; fax 0086-531-66658156; email xuguoxin1985@163.com (GX); Tel 0086-531-66658127; fax 0086-531-66652303; email wanshubo2016@163.com (SW))
[†]These authors contributed equally to this article.

Keywords: High-resolution, Peanut, Spatial transcriptome, Stereo-seq.

High-throughput single-cell RNA sequencing (scRNA-seq) technology has developed rapidly in recent years (Xie *et al*., 2022). However, due to differentiated cell types resistant to protoplasting, and cell spatial information restoration dependent on the well-studied marker genes and other reasons, which are limited the application of scRNA-seq in non-model species (Shaw *et al*., 2021). Peanut possesses a unique feature to embed its fertilized ovary into the soil through a specialized organ known as the peg, which has a stem-like morphology and anatomy but behaves like a root with positive gravitropism (Moctezuma, 2003). Here, we successfully established the SpaTial Enhanced REsolution Omics-sequencing (Stereo-seq) in this species and revealed the complex cell type-specific and spatial gene expression features of the peg by comparison with other three tissues (root, stem and hypocotyl, which have some common anatomical structures).

Schematic representation of the Stereo-seq procedure for peanut tissues was shown in Figure 1a. Sample preparation, RNA-seq and data analysis were improved according to Chen *et al*. (2022). A two-step cryo-embedding method was developed to minimize the tissue contraction for sample preparation of roots, hypocotyls, stems and pegs. Cryo-sections at 10 μm thickness were mounted on the 100 mm^2 Stereo-seq chips designed for plant tissues. In the two-step permeabilization method, the solutions were sprayed on the section surface with an ultrasonic atomizer to avoid lateral diffusion of mRNA solution (see details in supplemental methods). The fluorescence intensity of *in situ* synthesized cDNA was significantly enhanced by the improved methods (Figures 1a and S1).

Totally, 1 347 263 645 valid raw reads and 938 764 561 clean reads were obtained from the chips of the four tissues. By aligning to Tifrunner genome, 35 970, 47 304, 47 096 and 44 825 genes were identified in roots, hypocotyls, stems and pegs, respectively. Based on the statistics of cell size and gene capture at bin size in four tissues (Tables S1, S2 and Figure S2), bin50-100 was used for further analysis, and the average unique molecular identifiers (UMIs) and gene number captured in the four tissues at bin80 is 1858 and 871, respectively, which is about half of that of single-cell sequencing technique (Zhang *et al*., 2019). The transcriptome profiles were projected in an unsupervised analysis by Seurat and the clusters were visualized by the uniform manifold approximation and projection (UMAP) (Stuart *et al*., 2019).

18 clusters (0–17) were visualized and their spatial distribution corresponding to the section structure was optimal at bin80 (Figure 1b). The epidermis and exodermis from hypocotyl and stem were clustered together as cluster11, while the epidermis and exodermis from roots and pegs were classified into cluster12, 2 and 13, respectively. The cortex regions from roots, hypocotyls, stems, and pegs were classified into cluster5, 1, 3 and 9, respectively. Notably, although the epidermis and exodermis of stem and hypocotyl were classified as the same cluster (cluster11), the UMAP showed the cluster11 can further be divided into two subclusters (Figure 1b). Dots of subcluster11-1 and 11-2 are from the stem and hypocotyl, respectively (Figure S3). We obtained 282 subcluster-enriched genes ($|log2| \geqq 0.25$) among the two subclusters. Gene ontology (GO) enrichment analysis showed that the enriched genes in subcluster11-1 were related to photosynthesis and carbon fixation, while those in subcluster11-2 were related to cell wall modification and plant pathogen resistance (Tables S3 and S4). These results are consistent with their development and adaptation to environments where stems require more carbohydrates for rapid growth, while hypocotyls require predominant expression of disease-resistant and cell wall genes to cope with plant diseases and stresses. Our data provided new insights into the cell heterogeneity in peanut, where the same type cells according to classical anatomy from different tissues may retain a high divergence of gene expression. For instance, the epidermis and exodermis from the tip of the pegs (cluster13) were separated from that of the basal part (cluster2). GO enrichment analysis showed that the enriched genes in cluster2 are mainly related to the stimulation of sensing environmental signals, which is consistent with the function divergence to respond to mechanical stimulus to initiate the ovule development. However, the cluster13 is related to the synthesis of glycoside and saponin, which may protect the ovules from underground pests (Table S5).

For the stem individually, nine cell clusters (S0-S8) were defined at bin75, which is optimally consistent with the distribution of cell type visualized in stem anatomy when restored (Figure 1c). Compared to bin80 (Figure 1b), cluster6 was further divided into 3 subclusters (S2, S5 and S7), cluster10 was divided into 2 subclusters (S4 and S6), which is more consistent with the stem anatomy of peanut. Ordering cells of the clusterS4-S7 by pseudo-time analysis revealed two-directional differentiation trajectory of cambium cells. As expected, most cells from clusterS7 (cambium cells) assembled at the beginning of pseudo-time, while xylem vessel and xylem

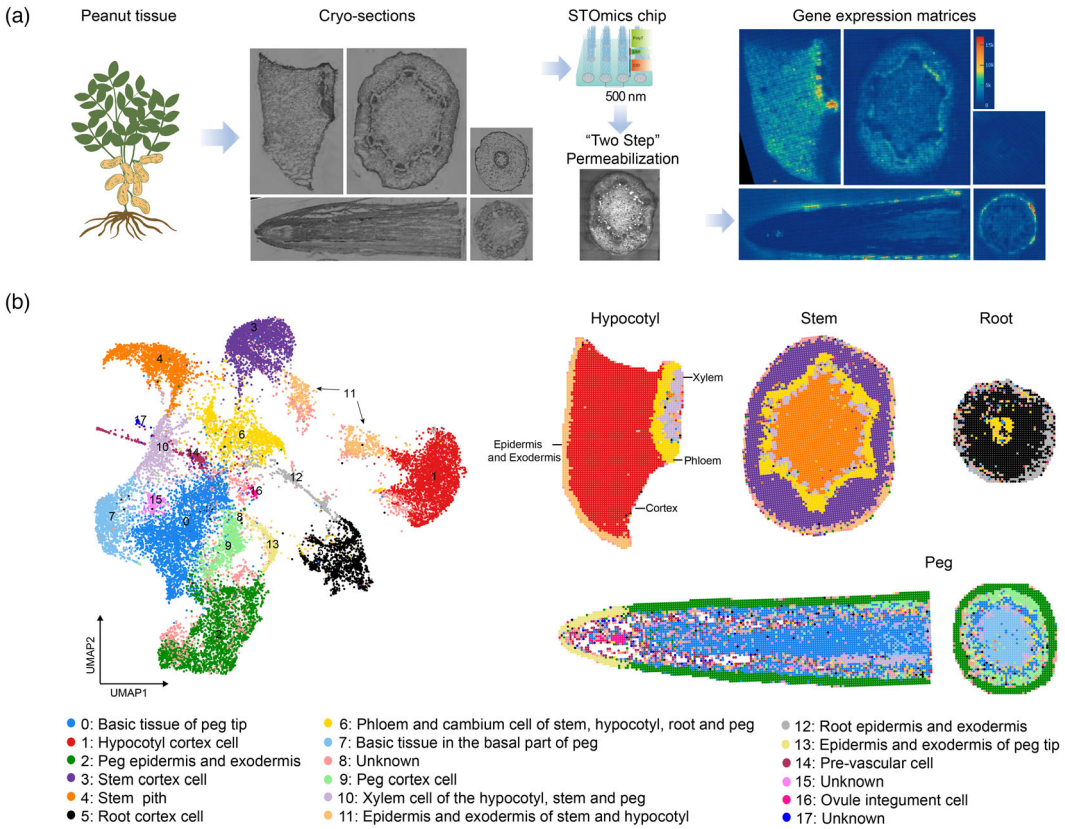

Figure 1 Spatial transcriptome maps of peanut tissues. (a) Schematic representation of the Stereo-seq procedure for peanut tissues. (b) Left, visualization of 18 cell clusters in peanut root, hypocotyl, stem and peg by UMAP. Right, the spatial distribution of each cluster was restored in the four tissues according to the CID sequence. (c) UMAP visualization of 9 cell clusters and their CID-based restored spatial distribution in stem section of peanut. (d) Monocle 3 analysis showing the cambium cells (S7) differentiated into xylem vessel and xylem parenchyma (S6 and S4) inward, and sieve element-companion cells (S5) outward. (e) The top 3 enriched genes (bottom) for each cluster. (f) Spatial expression pattern of nine representative enriched genes. The upper panel: *WAT1*, *CESA7*, *MLP43* in stems; the middle panel: *EXTENSIN3* in roots, *XTH1* and *ABR17* in hypocotyls; the bottom panel: *BBI1*, *MADS1* and *AGL5* in pegs.

parenchyma cells (S6 and S4) and sieve element-companion cells (S5) were grouped into different branches (Figure 1d).

Genes specifically expressed in one to two clusters were identified as cluster-enriched and the top 3 high enriched genes of each cluster were listed by using FindAllMarkers (Figure 1e and Tables S6, S7, Stuart *et al.*, 2019). For instance, three homologues of well-known marker genes *WALLS ARE THIN 1* (*WAT1*), cellulose synthase gene (*CESA7*), and xyloglucan endotransglucosylase/hydrolase 1 (*XTH1*) were identified as enriched in phloem parenchyma, xylem parenchyma, and epidermis and exodermis, respectively. Two MADS-box genes (*MADS1* and *AGL5*) were specially expressed in the ovules of the peg. Notably, some stress or disease resistance-related genes, including BURP domain protein RD22 (*RD22*), Bowman-Birk proteinase inhibitor 1 (*BBI1*), MLP-like protein 43 (*MLP43*), ABA-response gene (*ABR17*) were also identified as enriched in certain tissues/cell types that have not been reported previously (Figure 1f). The specific spatial expression patterns in the stem of 8 genes were verified by qPCR, which is consistent well with their cell anatomy classification (Figure S4). Furthermore, *MLP43* and *CESA7* were verified enriched in the xylem vessel and xylem parenchyma by *in situ* hybridization, respectively (Figures S4 and S5). These results showed that the spatial distribution of cell clusters is highly consistent with the cell anatomy classification.

Overall, combining the improved cryo-embedding and permeabilization strategy, we established a high-resolution spatial transcriptome atlas of partial single-cell level by the Stereo-seq technology in a non-model species. Although the gene number captured in the four tissues is approximately half of that of single-cell sequencing technique; however, the more useful spatial information independent of marker genes makes sense in particular to the non-model species. The high-resolution *in situ* transcriptome can avoid the disadvantages of single-cell sequencing and apply to non-model species, which will shed light on functional genomics studies at nano/micro-scale resolution level and lay solid transcriptomic strategy for further studies on biological problems in peanuts and other plants.

Acknowledgement

This work was supported by programs from NSFC (31871665), the Shandong Provincial programs (YDZX20203700001861, 2021LZGC026).

Conflict of interest

The authors declare no conflict of interest.

Author contributions

G.L., G.X. and S.W. designed the experiments. G.X., C.L., Y.L., Y.H., X.S. and F.C. performed the experiments. C.L., H.Z., X.L. and R.L. performed bioinformatics analysis. G.L., Y.L., S.W. and G.X. wrote the manuscript. All the authors read and approved the manuscript.

Data availability statement

The codes were deposited in Figshare (DOI:10.6084/m9.figshare.20097713), and the original data and expression matrix were deposited in CNGB database (https://www.cngb.org/) with CNP0002814.

References

Chen, A., Liao, S., Cheng, M., Ma, K., Wu, L., Lai, Y., Yang, J. *et al.* (2022) Largefield of view-spatially resolved transcriptomics atnanoscale resolution. *Cell* **185**, 1777–1792.

Moctezuma, E. (2003) The peanut gynophore: a developmental and physiological perspective. *Can. J. Bot.* **81**, 183–190.

Shaw, R., Tian, X. and Xu, J. (2021) Single-cell transcriptome analysis in plants: advances and challenges. *Mol. Plant* **14**, 115–126.

Stuart, T., Butler, A., Hoffman, P., Hafemeister, C., Papalexi, E., Mauck, W.M., III, Hao, Y. *et al.* (2019) Comprehensive integration of single-cell data. *Cell* **177**, 1888–1902.

Xie, J., Li, M., Zeng, J., Li, X. and Zhang, D. (2022) Single-cell RNA sequencing profiles of stem-differentiating xylem in poplar. *Plant Biotechnol. J.* **20**, 417–419.

Zhang, T., Xu, Z., Shang, G. and Wang, J. (2019) A single-cell RNA sequencing profiles the developmental landscape of Arabidopsis root. *Mol. Plant* **12**, 648–660.

Supporting information

Additional supporting information may be found online in the Supporting Information section at the end of the article.

Figure S1 Fluorescence intensity of in situ synthesized cDNA on peg cross-sections. (a) Previous permeabilization method according to Chen *et al.* (2022). (b) Improved permeabilization method. Bar = 500 μm.
Figure S2 Statistics of cell size in four tissues were investigated.
Figure S3 Visualization of subcluster11–1 and 11–2 by UMAP.
Figure S4 Gene spatial distribution, stem dissection and gene expression analysis by qPCR in stems.
Figure S5 In situ hybridization of MLP43 and CESA7 in peanut stem.
Table S1 Statistics of the cell size in four tissues investigated.
Table S2 Statistics of Gene and UMI number in four tissues investigated.
Table S3 Subcluster-enriched genes in subcluster11-1 and 11-2.
Table S4 TOP 5 GO items of enriched genes in subcluster11-1 and subcluster11-2.
Table S5 Top 5 biological processes from GO in terms of the enriched genes in 18 clusters.
Table S6 Enriched genes in 18 clusters of four tissues.
Table S7 Cell type-specific enriched genes were identified in stems, hypocotyls, roots and pegs.
Appendix S1 Supplementary material.

